

Simultaneous Determination of Flow Stress and Interface Friction by Finite Element Based Inverse Analysis Technique

H. Cho¹, G. Ngaile¹

¹Engineering Research Center for Net Shape Manufacturing

The Ohio State University, Columbus, OH, USA

Submitted by T. Altan (1), Columbus, USA

Abstract

A finite element based inverse analysis technique has been developed to determine the flow stress and friction at the tool/workpiece interface simultaneously from one set of material tests. The inverse problem is aimed at minimizing the error between experimental data and predictions made by rigid-plastic finite element simulations. The ring compression test and the modified limiting dome height test (sheet blank with a hole at center stretched with a hemispherical punch) were selected for evaluating the method for bulk forming and for sheet forming, respectively. The determined flow stress data were compared with corresponding data obtained independently using the well-lubricated cylinder compression test and hydraulic bulge test. Results show that the method discussed in the study is efficient and accurate.

Keywords:

Finite element method (FEM), Material, Inverse Analysis

1 INTRODUCTION

The finite element simulation of metal forming processes has been widely used to predict metal flow and to optimize the manufacturing operations. Today in using user-friendly commercial FEA software it is necessary to assign input parameters for the simulation. Among those inputs, the parameters in the flow stress equation, friction factor, and anisotropy coefficients of a material are usually obtained from the appropriate tests. However, since the results of process simulation are extremely sensitive to the accuracy of flow stress and interface friction that are input to FEM programs, it is essential that these input values are determined using (1) reliable material tests and (2) accurate evaluation methods.

A test used to determine material properties should replicate processing conditions that exist in practical applications. A common method for the determination of the flow stress data for bulk metal forming simulation is the upsetting test because (a) during the test the deformation is done in a state of compressive stress, which represents well the true stress state of most bulk metal forming processes and (b) the test can be done for a large strain. In this sense, for sheet metal forming where the biaxial stress state is dominating, a test similar to the limiting dome height test can provide more reliable data than the tensile test.

Also, the evaluation of the test results should be able to overcome difficulties introduced by friction and inhomogeneous deformation. Even in the simple cylinder upset, interface friction leads to an inevitable bulging of the sample and thereby to an inaccurate flow stress determination. Thus, it is better to consider the unavoidable friction at the tool/workpiece interface in the test and to identify it together with flow stress using the inverse analysis. Therefore, the accurate determination of the input parameters for FEM simulation, including material parameters in flow stress model and friction at the tool/workpiece interface, becomes a crucial research area in FEA.

In recent years, an inverse analysis technique combining the FEM with an optimization algorithm to identify

material parameters for metal forming process simulation has been introduced [1]. In the inverse analysis, the unknown parameters are determined by minimizing a least-square functional consisting of experimental data and FEM simulated data. The FEM is used to analyze the behavior of the material during the test, whereas the optimization technique allows for automatic adjustment of parameters until the calculated response matches the measured one within a specified tolerance.

In this study, based on rigid-plastic finite element formulation, a new inverse analysis algorithm has been formulated and a methodology for simultaneous determination of flow stress and interface friction has been introduced. In order to verify the developed inverse analysis algorithm, the load-stroke curve and the measured geometry change, which are sensitive to interface friction, were used as experimental input data in the inverse analysis. The ring compression test was selected for evaluating the method for bulk forming while the modified limiting dome height test was developed for testing the method in sheet forming because (a) the stress state in both tests can reflect well the prevailing stress state in the actual process and (b) changes in the internal diameter of rings and changes in hole diameter of sheet are dependent on the tribological condition.

2 INVERSE ANALYSIS ALGORITHM

2.1 Algorithm for flow stress determination

The basic concept of an inverse analysis for parameter identification is to compute a set of unknown material parameters \mathbf{p} , which represents the flow stress curve. The unknown parameters are determined by minimizing an objective function, $E(\mathbf{p})$, representing the difference between the experimental and corresponding computed loads in a least-square sense:

$$E(\mathbf{p}) = \frac{1}{N} \sum_{i=1}^N \left(\frac{F_i - f_i(\mathbf{p})}{F_i} \right)^2 \quad (1)$$

where F is the experimentally measured load and f is the computed load. N is the number of data sampling points in a load vs. stroke curve used to construct the objective function. For a given set of material parameters, the objective function will be minimum at:

$$\frac{\partial E(\mathbf{p})}{\partial p_k} = 0 \quad \text{for } k = 1, \dots, m \quad (2)$$

where m is the number of parameters to be identified.

The equation (2) is solved with respect to the parameters p_k using Newton-Raphson iterative method.

$$\frac{\partial^2 E}{\partial p_k \partial p_j} \Delta p_j = -\frac{\partial E}{\partial p_k} \quad \text{for } k, j = 1, \dots, m \quad (3)$$

The first and second derivatives of the objective function with respect to the parameters p_k are evaluated by taking the derivatives of Equation (1) with respect to material parameters p_k :

$$\frac{\partial E}{\partial p_k} = -\frac{2}{N} \sum_{i=1}^N \left\{ \frac{(F_i - f_i)}{F_i} \frac{\partial f_i}{\partial p_k} \right\} \quad (4)$$

$$\frac{\partial^2 E}{\partial p_k \partial p_j} = -\frac{2}{N} \sum_{i=1}^N \left\{ -\frac{\partial F_i}{\partial p_k} \frac{\partial f_i}{\partial p_j} + (F_i - f_i) \frac{\partial^2 f_i}{\partial p_k \partial p_j} \right\} \quad (5)$$

where the computed force f_i is defined in rigid-plastic FEM as follows [2]:

$$f_i = \sum_e \int_{V^e} \frac{2}{3} \frac{\bar{\sigma}}{\bar{\epsilon}} \mathbf{B}^T \mathbf{D} \mathbf{B} dV \hat{\mathbf{v}} + \sum_e \int_{V^e} \mathbf{G} \mathbf{B}^T \mathbf{c} \mathbf{c}^T \mathbf{B} dV \quad (6)$$

$\bar{\sigma}$ is the effective stress, which is equal to the flow stress of material during the plastic deformation, $\dot{\bar{\epsilon}}$ is the effective strain rate, \mathbf{B} is the strain rate-nodal velocity matrix, and \mathbf{G} is the penalty constant respectively. \mathbf{D} and \mathbf{c} are a matrix and a vector of constant components.

Thus, f_i , $\frac{\partial f_i}{\partial p_k}$, and $\frac{\partial^2 f_i}{\partial p_k \partial p_j}$ are calculated using Equations (6)-(8) only for tool-contacting elements.

$$\frac{\partial f_i}{\partial p_k} = \sum_e \int_{V^e} \frac{2}{3} \frac{1}{\bar{\epsilon}} \left(\frac{\partial \bar{\sigma}}{\partial p_k} \right) \mathbf{B}^T \mathbf{D} \mathbf{B} dV \hat{\mathbf{v}} \quad (7)$$

$$\frac{\partial^2 f_i}{\partial p_k \partial p_j} = \sum_e \int_{V^e} \frac{2}{3} \frac{1}{\bar{\epsilon}} \left(\frac{\partial^2 \bar{\sigma}}{\partial p_k \partial p_j} \right) \mathbf{B}^T \mathbf{D} \mathbf{B} dV \hat{\mathbf{v}} \quad (8)$$

For a strain hardening material, the flow stress equation may be given by $\bar{\sigma} = K \bar{\epsilon}^n$. The first and second derivatives of the flow stress equation with respect to material strength constant K and strain hardening index n are expressed by Equation (9).

$$\frac{\partial \bar{\sigma}}{\partial p_k} = \left\{ \frac{1}{K} \bar{\sigma} \right\}, \quad \frac{\partial^2 \bar{\sigma}}{\partial p_k \partial p_j} = \begin{bmatrix} 0 & \frac{\ln \bar{\epsilon}}{K} \bar{\sigma} \\ \frac{\ln \bar{\epsilon}}{K} \bar{\sigma} & (\ln \bar{\epsilon})^2 \bar{\sigma} \end{bmatrix} \quad (9)$$

The optimal amount of adjustments for material parameters Δp_k is found after solving Equation (3). Then

material parameters are improved iteratively until Equation (2) is satisfied using the following equation.

$$p_k^{(i+1)} = p_k^{(i)} + \Delta p_k \quad (10)$$

At the next optimization step a new FEM simulation is conducted with improved material parameters and this procedure is repeated until the deviation of material parameters becomes within tolerance. The flow chart of this algorithm is shown in Figure 1.

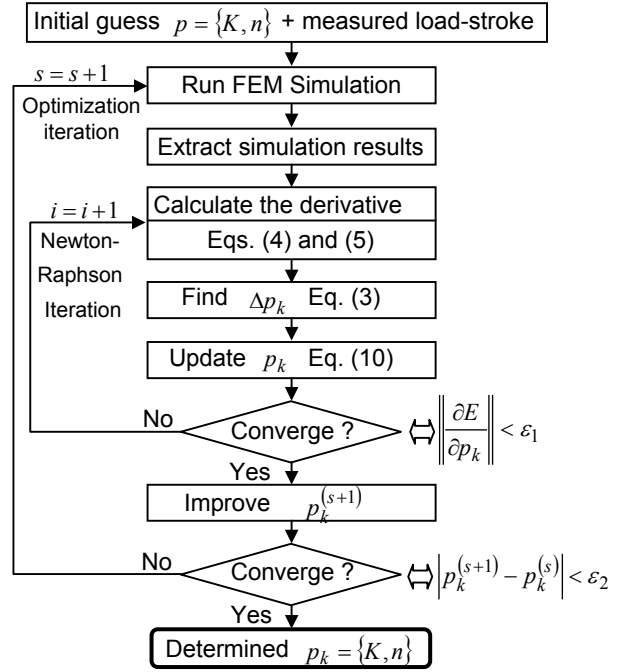


Figure 1: Flow chart of inverse analysis.

2.2 Procedure for flow stress and friction determination

In the FEA of metal forming process, it is assumed that the tribological conditions at the tool/wprkpiece interface can be modeled either by constant shear friction model or by Coulomb friction model represented by Equations (11) and (12), respectively.

$$\tau_f = m_f k \quad \text{for bulk metal forming} \quad (11)$$

$$\tau_f = \mu p \quad \text{for sheet metal forming} \quad (12)$$

where τ_f is the frictional shear stress, p is the surface pressure and k is local yield stress. Generally the friction factor, m_f , and the friction coefficient, μ , are assumed to remain constant during the metal forming process. The frictional force affects the metal flow. Therefore, the shape of the deformed specimen is sensitive to interface friction. Thus, by comparing the experimentally measured shape of the part and its corresponding computed shape, the unknown friction factor (or coefficient) can be identified inversely.

For determining the flow stress and the interface friction simultaneously from one set of tests, the following objective function can be considered:

$$E(p, m_f) = \frac{1}{N} \sum_{i=1}^N \left(\frac{F_i - f_i(p, m_f)}{F_i} \right)^2 + \sum_{i=1}^N (D_i - d_i(p, m_f)) \quad (13)$$

The objective function is a function of material parameters p_k and friction factor m_f . The first term represents the difference between the experimental and corresponding computed loads in a least-square sense as shown in Equation (1). The second term indicates the difference between the measured geometry and its corresponding computed geometry d . To find out a set of p_k and m_f that minimize Equation (13), several inverse analyses must be conducted by changing the friction factor. This procedure is repeated until both the first and second term in Equation (13) are minimized completely with respect to p_k and m_f as shown in Figure 2.

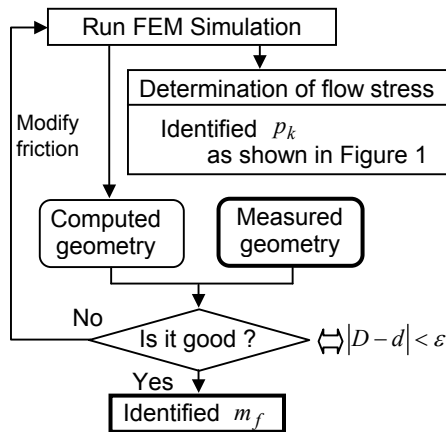


Figure 2: Flow chart for determination of flow stress and friction factor by the inverse analysis.

3 EXAMPLES OF INVERSE ANALYSIS

3.1 Ring compression test

Experiment

The developed inverse analysis algorithm has been tested by using the real experimental data obtained from compression of ring specimen of aluminum 6061-T6. Rings with 54 mm O.D. x 27 mm I.D. x 18 mm height were compressed at various reductions. The rings were coated by spraying Teflon spray on all surfaces of the samples and on the top and bottom dies. In order to observe internal diameter variation the test was stopped at reductions of 7.2, 22.2 and 40%. Figure 3(a) shows the compressed ring samples and Table 1 shows the decrease of I.D. of the ring at different reductions.

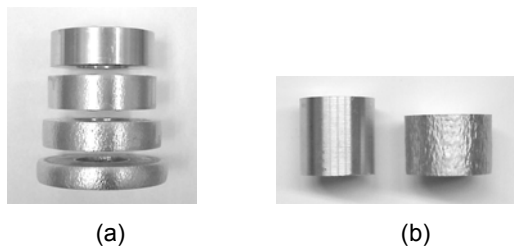


Figure 3: Compressed (a) ring and (b) cylinder samples.

Reduction in height [%]	Decrease in I.D. of ring [%]
7.2	-1.48
22.2	-2.96
40.0	-1.85

Table 1: Percent decrease in I.D. of ring.

Determination of flow stress and friction

The results of identified parameters (K-value and n-value) in the flow stress equation and friction factor by the inverse analysis are summarized in Table 2. Three inverse analyses were conducted by varying the friction factor from 0.15 to 0.2. As initial guesses of material parameters $K = 430(\text{Mpa})$ and $n = 0.1$ were used for every case. When the friction factor 0.175 was assumed, the inverse analysis prediction produced only 8.1% underestimation in I.D. comparison of the ring. Thus, a combination of friction factor $m_f = 0.175$ and flow stress $\bar{\sigma} = 452\bar{\epsilon}^{0.074}(\text{Mpa})$ gives the best minimum for the objective function. As can be seen in Figure 4, after four optimization iteration, computed and experimental loads are nearly identical.

Friction m_f	Decrease in I.D. of ring [%]	K-value (Mpa)	n-value
0.2	+0.5	446	0.073
0.15	-5.9	459	0.076
0.175	-1.7	452	0.074

Table 2: Predicted inverse analysis results.

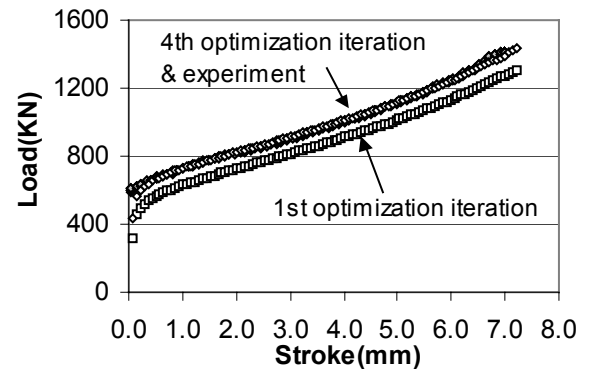


Figure 4: Comparison of computed and experimental load-stroke curves (ring test).

Verification of the determined friction factor

To verify the accuracy of determined friction factor, FEM simulations using the determined flow stress with friction factor of 0.175 were conducted for various friction factors. Thus, the ring calibration curves were generated as shown in Figure 5. It is seen that measurements match well the curve obtained with the friction factor of 0.182, which is very close to 0.175.

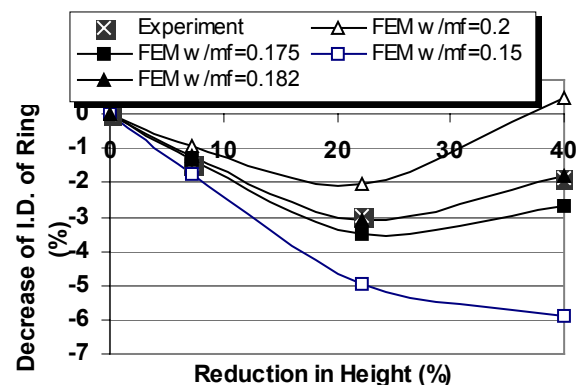


Figure 5: Ring calibration curves obtained with $\bar{\sigma} = 452\bar{\epsilon}^{0.074}(\text{Mpa})$.

Verification of the determined flow stress

In order to verify the flow stress determined with friction factor by the inverse analysis, the aluminium cylinders with a 30 mm dia. x 30 mm height were upset to 38% reduction in height. To minimize interface friction, the interface was lubricated with Ecoform lubricant made by Fuchs. As shown in Figure 3(b), the lubrication nearly eliminated bulging in upsetting of cylinder. Using the measured load-stroke curve, flow stress $\bar{\sigma} = 437\bar{\epsilon}^{0.067}$ (Mpa) was obtained. The difference between the flow stress data obtained in ring and cylinder compression tests is about 3.3% in K-value and 9.5% in n-value, respectively.

3.2 Modified limiting dome height test

Experiment

In this test a hole with the diameter of 8mm was drilled at the center of cold rolled AKDQ sheet specimen with 0.86 mm thickness. The sheet is then stretched over a 152 mm diameter hemispherical punch. The radius of upper die is 50 mm. The press ram velocity of 60 mm/s was used. Three specimens were tested for lubricant A and B. Due to the fact the holes weren't exact circles after the test, it was necessary to take an average from different measuring points of the deformed hole. The stroke was limited to 44 mm to avoid any fracture. Figure 6 shows a sketch of the modified limiting dome height test and Figure 7 shows the tested specimens.

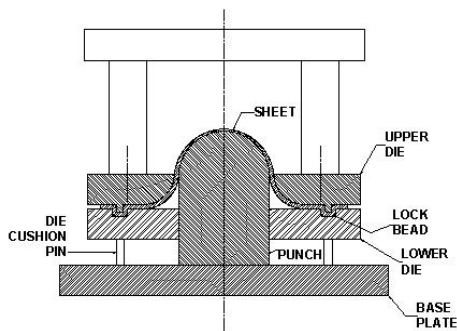


Figure 6: Modified limiting dome height test.



Figure 7: Initial and tested specimens for Lub. A and B.

Lubricant	Measured hole diameter [mm]	Measured max. load [kN]
A	15.40	56
B	16.59	53

Table 3: Hole expansion and maximum punch force.

Determination of flow stress and friction

Using the load-stroke curve and measured hole diameter at the final stroke, several inverse analyses were conducted by varying the friction coefficient from 0.05 to 0.4 for lubricants A and B. 10 data sampling points were taken from each load-stroke curve. As summarized in Table 3 and Table 4, the measured hole diameter and corresponding inverse analysis prediction showed a good agreement. The friction coefficient 0.15 was identified for lubricant A and 0.08 was identified for lubricant B. It is noteworthy that, while these two different lubricants gave

two different friction coefficients, the determined K and n values are almost identical. This result is expected since sheet material was the same in both tests.

Lubricant	Friction Coef.	Hole dia. [mm]	K-value (Mpa)	n-value	Load [kN]
A	0.15	15.35	646	0.174	56
B	0.08	16.54	645	0.174	54

Table 4: Predicted inverse analysis results after 20 optimization iterations.

The hole expansion values obtained from the modified limiting dome height test can also be used to rank the lubricants. A larger hole expansion indicates a better performance of the lubricant used.

Comparison of the flow stress with available data

To further evaluate the accuracy of the flow stress data obtained by inverse analysis a comparison was made with published information. Table 5 gives the coefficients K and n of the flow stress equation ($\bar{\sigma} = K\bar{\epsilon}^n$), determined by inverse analysis, with corresponding values obtained in an earlier study [3]. This comparison indicates that the predictions made with the method, developed in the present study, are comparable to results obtained directly with bulge tests, conducted in an earlier investigation.

Coefficient	Inverse Analysis	Reference [3]	Difference (%)
K (Mpa)	646	689 ~ 724	6.6 ~ 12.1
n	0.174	0.17 ~ 0.23	2.3 ~ 32.2

Table 5: Comparison of predicted flow stress coefficients for AKDQ steel with data generated by Gutscher et al [3].

4 CONCLUSIONS

An inverse analysis that combines the finite element method and the optimization algorithm has been developed to determine flow stress and interface friction simultaneously. As examples inverse analyses of the ring compression and the modified limiting dome height tests were conducted. The results indicated that with this method it was possible to predict the flow stress and friction with acceptable accuracy.

5 ACKNOWLEDGEMENTS

The authors gratefully acknowledged the support from the NSF grant No. 0010008 entitled "Improvement of Tribological Conditions in Tube Hydroforming by using Environmentally Friendly Lubricant Systems and Textured Tubes". The authors also thank Prof. Naksoo Kim of Sogang Univ., Korea for his valuable suggestions.

6 REFERENCES

- [1] Chenot, J.-L., Massoni, E., Fourment, L., 1996, Inverse Problems in Finite Element Simulation of Metal Forming Processes", Engineering Computations, Vol. 13, No. 2/3/4, p. 190-225.
- [2] Kobayashi, S., Oh, S.-I., Altan, T., 1989, Metal Forming and Finite Element Method, Oxford University Press, NY
- [3] Gutscher, G., W, H.-C., Ngaile, G., Altan, T., 2000, Evaluation of Formability and Determination of Flow Stress Curve of Sheet Metals with Hydraulic Bulge Test, Report No. S/ERC/NSM-00-R-15, ERC/NSM, USA